Journal of Fluorescence
https://doi.org/10.1007/s10895-020-02645-5

ORIGINAL ARTICLE

Green Synthesis of Fluorescent Carbon Dots from *Elaeagnus angustifolia* and its Application as Tartrazine Sensor

Mahnaz Ghereghlou[1] · Abbas Ali Esmaeili[1] · Majid Darroudi[2,3]

Received: 3 September 2020 / Accepted: 30 October 2020

Abstract

This article has introduced and examined a novel and green approach for the very first time, which had been developed for the synthesis of carbon dots (CDs) and performed through the utilization of *Elaeagnus angustifolia* (E. A) as a natural carbon source. This straightforward procedure has been based upon a hydrothermal treatment with a quantum yield of 16.8% that had been designed to synthesize water-soluble CDs in one step and result in a satisfying fluorescence. Additionally, we have attempted to assess the sensing system that had been exerted through the usage of CDs for the detection of food colorant tartrazine, since they can function as a fluorescent sensor due to the interplay that occurs among tartrazine and CDs leading to the quenching of their fluorescence. The detection limit has been measured to be equaled to 0.086 μM (86 nM) and the linear range has been observed to be 0.47–234 μM. The proposed highly sensitive and simple method has exhibited an excellent selectivity and proved to be effectively applicable for distinguishing the tartrazine of real samples.

Keywords Green synthesis · Carbon dots (CDs) · *Elaeagnus angustifolia* · Tartrazine · Hydrothermal

Introduction

Carbon dots (CDs), also known as carbon nanodots or carbon quantum dots, have been recently added to the family of fluorescence carbon nanoparticles. Which had been discovered through the work of Xu et al. in 2004 [1, 2]. The typical size of CDs is ranged under 10 nm and normally detected in discrete, quasi-spherical, nanocrystalline, or amorphous carbon structural shapes [2]. According to observations, CDs contain sp^2/sp^3 carbon and are composed of either oxygen/nitrogen-based groups or polymeric aggregations. Among the different methods that had been developed for the synthesis of carbon dots, the most common techniques are the "top-down" cutting from varying carbon sources and "bottom-up" synthesis through organic molecules or polymers [3].

Considering how the bottom-up organic processes involve dehydration and carbonaceous aggregation by the usage of small molecules that are labeled as precursors, however, it is also possible to synthesize CDs from organic and non–toxic precursors including carbohydrates [4]. Although the synthesis of CDs through the bottom-up approach demand the application of small/big precursor-molecules similar to carbohydrates and organic acids such as citrates, natural products, and etc., nevertheless, certain processes including hydrothermal, solvothermal, chemical, plasma treatments, and microwave synthesis are required to be engaged as well [5].

Relatively, the hydrothermal methods have proven to be cheap, eco-friendly, and non-toxic that require high temperatures and high pressure within an autoclave system. However, CDs can be produced without calling for drastic conditions [6]. In recent years, the development of green and uncomplicated synthesizing methods for producing high fluorescent CDs has gathered the focus of researchers and in this regard, several reports have attempted to perform green methods through the usage of inexpensive plant extracts, fruit juices, garlic, vegetables, and edible waste to function in the position of carbon precursors [7–10].

✉ Abbas Ali Esmaeili
abesmaeili@fum.ac

✉ Majid Darroudi
darroudim@mums.ac.ir; majiddarroudi@gmail.com

[1] Department of Chemistry, Faculty of Sciences, Ferdowsi University of Mashhad, Mashhad, Iran

[2] Nuclear Medicine Research Center, Mashhad University of Medical Sciences, Mashhad, Iran

[3] Department of Medical Biotechnology and Nanotechnology, School of Medicine, Mashhad University of Medical Sciences, Mashhad, Iran

Published online: 16 November 2020

The fabrication of CDs through the usage of fruits is commonly carried out by hydrothermal synthesis. Due to their superior fluorescent properties, CDs are commonly investigated as fluorophores to be applied for the sensitive and selective detection of different substances. In addition, they have a high potential for fluorescence-based analytical applications because of their simple preparation, water-solubility, and requiring low-costs [11–13]. Consequently, these features can facilitate a better food quality and safety detection by providing a highly sensitive and selective behavior [14]. E.A., commonly known as oleaster or Russian olive, belongs to the genus Elaeagnus of Elaeagnaceae species. The tree of this small reddish-brown elliptic fruit has been observed to grow throughout Asia, Europe, and North America. The Oleaster fruits can stand as rich sources of proteins, carbohydrates, vitamins, minerals, phenolic compounds, antioxidants, and fibers [15]. The E.A. grows naturally in Iran and its Oleaster fruits, which are called "Senjed" in local vernacular, are used for local consumption and marketing [16]. However, this substance has been exerted as a new source of carbon for performing the synthesis of CDs, which are meant to be applied for the detection of a certain synthetic food dye, known as Tartrazine (3-carboxy-5-hydroxy-1-(4′-sulfophenyl)-4-(4′-sulfophenyl) azo) pyrazole trisodium salt). The regular engagement of Tartrazine in the production of foodstuffs and soft drinks results in enhancing their appearance, color, and texture, as well as preserving their natural color in the courses of being prepared or stored [17]. There are certain advantages in selecting the usage of synthetic dyes over natural dyes, including their high stability in light, oxygen, and pH, which explains the existing tendency towards the utilization of synthetic paints instead of natural colors [18]. The excessive application of tartrazine has proved to cause adverse effects on human health [19] which include chronic toxicity, migraines, diarrhea, and carcinogenicity [20]; therefore, it can be indicated that the levels of appended color to editable products must be carefully measured. Relatively, many countries have banned and strictly controlled the utilization of tartrazine dyes in foodstuff and drinks [21]. Although a large number of analytical methods for the routine monitoring of tartrazine have been proposed, such as spectrophotometric, chromatography [22–24], and electrochemical determination [25, 26], yet only a few of them have proved to be practical while requiring time-consuming and complicated processes, as well as costly instruments and environmentally unfriendly conditions. Considering the mentioned facts, the accelerating need for discovering other techniques that would be relatively less problematic can be thoroughly perceived. Fluorescent carbon spots that had been derived from automobile exhaust soot have been used for the regulation of Tartazine in soft drinks [27, 28]. Meanwhile in another study, N, Cl Co-doped fluorescent carbon dots have been applied as nanoprobe to detect the existence of this synthetic dye in beverages [29].

In this work, we have proposed a simple, low-cost, and green method for the synthesis of fluorescent CDs, which had been done through the hydrothermal treatment of E.A., as a new carbon precursor (Fig. 1). Based on the observed high-level of photoluminescence in the obtained CDs, a fluorescent-based probe has been designed in which they are applied for the detection of tartrazine. Next to being simple, eco-friendly, and cost-effective, the proposed method has turned the thought of effortless synthesis into a possible approach that does not require the addition of any chemical reagents.

Experimental

Chemicals and Materials

We have procured E.A., form a local market in Mashhad, Iran, while all the other reagents and chemicals had been purchased from Sigma–Aldrich (USA) and Merck (Darmstadt, Germany). The involved chemicals and reagents have been ascertained to be of analytical grade without requiring any further purification. As the last ingredient, deionized water has been also exerted in the course of the experiment. Initially, the specified portion of tartrazine has been dissolved in double-distilled water to prepare the needed stock standard solution (1.0×10^{-3} μg. mL^{-1}). We have also composed the working mixtures of lower concentrations in a daily basis through the dilution of stock solution with double distilled water. In addition, a Britton-Robison (B-R) buffer along with varying pH values have been formulated, which had been done by appending the distinct portions of 0.2 M of NaOH to 0.04 M of acetic acid, boric acid, and phosphoric acid mixtures.

Apparatus

We have distinguished the sizes and frameworks of the obtained CDs through the employment of transmission electron microscopy (TEM, Hitachi-600, Hitachi, Japan) and in order to record the UV − Vis absorption spectra, a double-beam UV − Vis spectrophotometer with the quartz cell of 1.0 cm has been exerted (Varian, Cary 1E, Australia). Furthermore, we have gathered data on the Fluorescence emission spectra through the utilization of a RF-5301PC spectrofluorometric that had been equipped with a 5.5 nm slit width (Shimadzu, Kyoto, Japan). Moreover, Fourier transform infrared (FTIR) spectra have been obtained on a Nicolet Nexus Fourier transform infrared spectrometer by the application of KBr pellets, as well as the usage of scans that had been prepared from 4000 to 500 cm^{-1} at room temperature with a resolution of 4 cm^{-1} and 16 scans. We have also investigated the interlayer spacing and amorphous nature of CDs by the means of X-ray

Fig. 1 Schematic illustration of synthesizing CDs based on *Elaeagnus angustifolia*

Diffractometer (XRD, GNR- EXPLORER, Italy), while the zeta potential had been measured through a Horiba (SZ-100, Japan).

Synthesis of CDs

In order to begin the process, the E.A had to be initially dried in air while being shaded. The typical, uncomplicated, and one-pot hydrothermal procedure that had been introduced for the synthesis of CDs has been designed as the following: First, we have peeled the E.A., and had thoroughly pulverized the separated pulp until obtaining a soft and uniformed powder. Then, 2.0 g of the powder has been appended to 30 mL of ultrapure water, which had been then stirred for 1 h to achieve a homogenous dispersion. Once the obtained mixture had been conveyed into a 50 mL Teflon-lined autoclave, it has been tightly sealed and heated at the temperature of 180 °C for the period of 12 h. As the next step, the autoclave has been put aside to be cooled off to room temperature and afterwards, recovered a brown crude solution that had to be sonicated for 20 min to achieve a homogenous dispersion. In order to dispatch the larger bulk particles and gather a clear yellow mixture, we had to centrifuge the dispersed solution at 10,000 rpm for 30 min; the yellow resultant has been filtered by the usage of a 0.22 μm MCE filter membrane. Lastly, the acquired two dispersions have been decided to be freeze-dried, which had resulted in the creation of light-brown residues that has been stored in dark at 4 °C for future application.

Detection of Tartrazine Using CDs

Initially, 100 μL of tartrazine solutions or sample solutions have been added into 100 μL of CDs aqueous dispersion. Subsequently, we have employed a Britton-Robinson (B-R) buffer of pH 6.0 to dilute the solutions into 3.0 mL and have them mixed afterwards with a vortex for 1 min. At last, the mentioned solutions have been incubated at a suitable temperature for 20 min and the procedure had been continued by recording the fluorescence spectra of mixtures through fluorometric analysis, involving the application of a 1 cm path length quartz cell under the fluorescence excitation wavelength of 330 nm and a slit width of 5 nm. We have calculated the fluorescence quenching efficiency as F0-F/F, in which F represents the fluorescence emission intensity of reaction system and F0 stands for blank.

Quantum Yield Measurement

The Fluorescence quantum yield (QY) of obtained CDs have been determined based on the applied slope method and in accordance with the following Eq. 1 [30]:

$$\Phi_X = \Phi_{ST}(Grad_x/Grad_{ST})\left(\eta^2 X/\eta^2 ST\right) \quad (1)$$

In which the subscripts ST and X stand for anthracene and carbon dot aqueous solutions, respectively. In addition, Φ would be the fluorescence quantum yield, Grad represents gradient from the plot of integrated fluorescence intensity vs absorbance, and η is the refractive index of solvent. It should be also noted that anthracene in ethanol has been applied as a standard ($\Phi_{ST} = 27\%$ at 360–480 nm) [31].

In order to calculate the quantum yield, we have prepared six concentrations of C-dots and anthracene while keeping their absorbance under 0.1, since there is a chance of observing non-linear effects in higher levels due to the impacts of inner filter, which could possibly result in perturbing the values of quantum yield. Anthracene with QY = 0.27 has been dissolved in ethanol (refractive index (η) of 1.36) while the C-dots had been mixed with ultrapure water (η = 1.33). Thereafter, we have recorded the fluorescence spectra and absorbency values at the excitation point of 330 nm. as well as plotting the graph of integrated fluorescence intensity vs absorbance that resulted in a straight line. The outcomes of calculating $Grad_X/ Grad_{ST}$, η^2_X/η^2_{ST}, and the Quantum yield of C-dots have been observed to be 65.0588, 0.9564 and 16.8%, respectively.

Results and Discussion

Characterization of CDs

The XRD pattern (Fig. 2a) of CDs within the range of 10–70° (2θ range) has exhibited a broad peak at 2θ = 25.46°, which had been in correlation to the designated (002) peak (JCPDS No. 26–1076) [32, 33]. This observation is suggestive of the interlayer spacing (d) of CDs at 3.49 nm and approves the weak crystalline nature of carbon dots, as well as indicating the amorphous nature of C-dots [34]. The existence of different functional groups in the CDs have been determined through the FT-IR spectroscopy technique (Fig. 2b). The CDs that had been synthesized in ultrapure water solutions have been dried under the conditions of freeze-drying to be

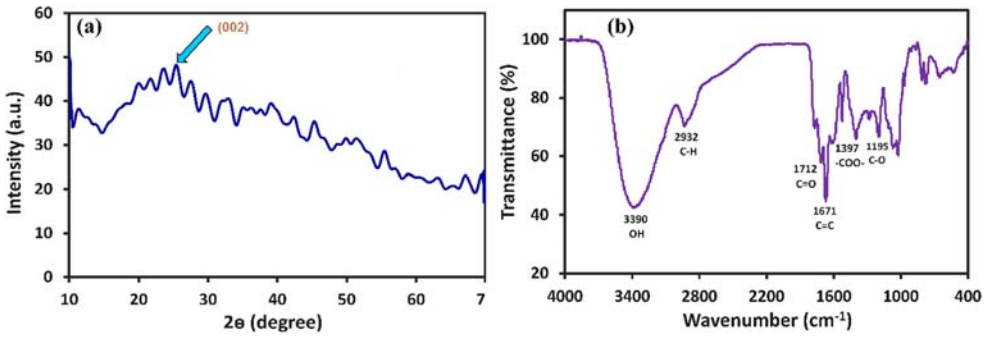

Fig. 2 (**a**) XRD pattern and (**b**) the FTIR spectrum of the as-synthesized CDs

analyzed. In regard to the FT-IR spectrum, the recorded peaks at 3390, 2932, 1712, 1671, 1397, 1195 cm^{-1} have referred to the appearances of –OH, –C–H, C=O, C=C, –COO−, and C–O, respectively [35, 36]. According to the TEM analysis (Fig. 3), the obtained CDs have been highly dispersible in aqueous solution with spherical morphology and had contained a narrow size below 10 nm [37].

Optical Properties of CDs

We have determined the optical features of prepared CDs through the utilization of UV–Vis absorption spectra and fluorescence emission spectra [38]. The UV–Vis spectra of synthesized carbon dots (Fig. 4) have exhibited a maximum absorption at 282 nm that had been assumed to be associated with the n–π* and π–π* transition of –C=O bonds and the conjugated C=C bands, respectively. The previous researches, which had been done on carbon particles through cellulose-based carbonization, have reported similar results to our outcomes [32]. The Fluorescence spectrum of CDs have indicated that the optimal excitation and emission wavelengths had been positioned at the points of 330 and 410 nm, respectively. As it can be perceived in Fig. 5a, the maximum fluorescent emission peak has been conveyed towards a higher wavelength with an increase in the excitation wavelength from 310 nm to 410 nm (with 10 nm increment). In addition, we have observed the strongest emission spectrum at the excitation wavelength of 330 nm. It has been assumed from the obtained normalized spectra in Fig. 5b that the fluorescence emission of carbon dots functions in an excitation-dependent manner [37]. Next to evaluating the stability of CDs, the presented UV − Vis spectra in Fig. 6 have been recorded throughout different days. Accordingly, all of the four types of UV − Vis absorption spectra have exhibited a strong peak in the point of 282 nm and it is also considerable that the overlap of provided spectra had been acceptable. Therefore, our results have confirmed the lack of any significant changes throughout the UV–Vis spectra and the satisfying stability of the composed CDs after even 3 months has been reported with negligible alteration, which had been kept in a dark place at 4 °C.

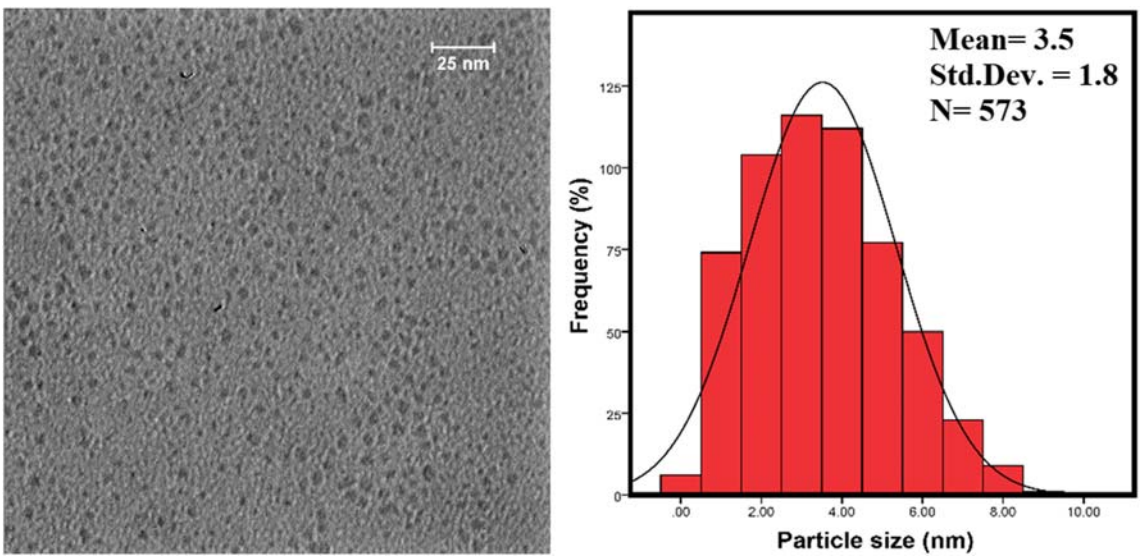

Fig. 3 TEM image of CDs from E.A and its corresponding size distribution

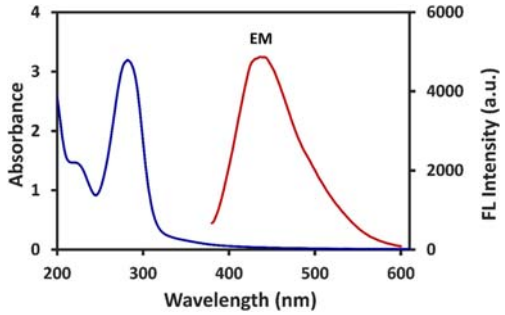

Fig. 4 UV-Vis absorption (blue curve) and Fluorescence emission (red curve) spectra for an aqueous solution of CDs

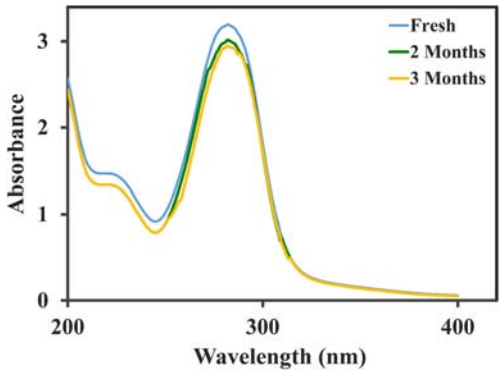

Fig. 6 The stability of CDs. Effect of storage time at 4 °C on UV-Vis absorption spectra

Optimization of Experimental Parameters

In prior to performing the quantitative analysis of tartrazine through the suggested sensing system, we have investigated the influences of media pH value and incubation time on fluorescence intensity in order to figure out the most effective conditions for detecting tartrazine (Fig. 7). According to Fig. 7a, and b, both of the mentioned parameters have caused an unnoticeable effect on the F0/F of this method, however, the reaction time of 20 min and pH = 6 have been settled for obtaining consistent outcomes. We have placed all of the involved samples at room temperature and had their fluorescence emission intensities recorded.

Detection of Tartrazine

We have appended different concentrations of tartrazine (0.47–234 μM) into CDs solution under the appointed conditions that had been mentioned above [39]. It has been indicated by the results that the fluorescence intensity of CDs has been quenched by tartrazine and as the concentration of this synthetic dye had been increased, the fluorescence intensity has been regularly decreased (Fig. 8a). As it is displayed, the linear relationship between the relative fluorescence responses (Fo/F) of CDs with different tartrazine concentrations can be observed. This particular relationship has been illustrated through the application of Stern-Volmer equation (Eq. (2)), which has proved to be the best in describing the quenching profile of fluorescence species that had been adopted:

$$F0/F = 1 + K_{SV}[Q] \tag{2}$$

in which F and F0 represent the fluorescence emission intensity of CDs with and without tartrazine, respectively, [Q] would be the concentration of tartrazine, and K_{SV} stands for the Stern–Volmer constant. The given calibration curve in Fig. 8b has exhibited a fine linear relationship y = 0.0028x + 0.0179 in the range of 0.47–234 μM, which had contained the correlation coefficient R^2 value of 0.9916. We have calculated the limit of detection (LOD) for tartrazine and obtained the value of 0.086 μM (86 nM). This measurement has been performed based on the equation of 3.3σ/k, in which σ represents the standard deviation of y-intercepts in regard to the regression lines and k stands for the slope of calibration graph, which had been comparable to the other reported values obtained through alternative methods [40–42].

The Quenching Mechanism of the Proposed Sensor

Under hydrothermal conditions, as well as high temperature and pressure, the carbohydrates of E.A., has been initially

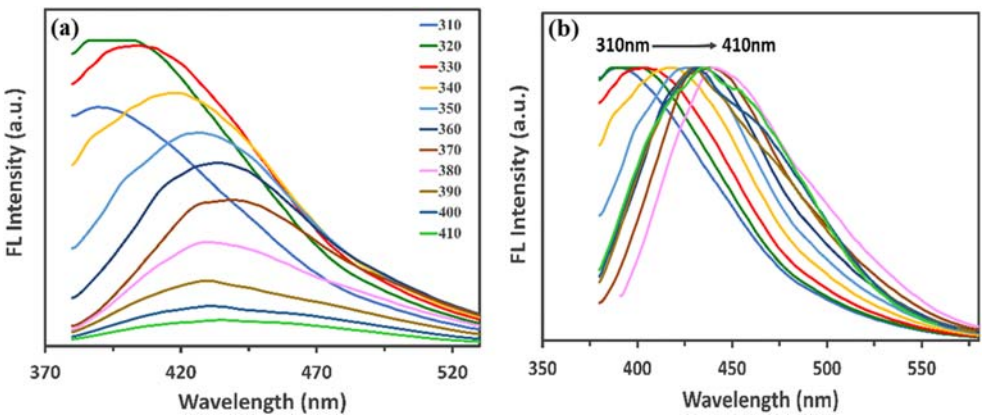

Fig. 5 (**a**) Fluorescence emission spectra of CDs at different excitation wavelengths from 310 to 410 nm in 10 nm increments and (**b**) The normalized FL spectra of CDs at λ_{ex} = 310–410 nm

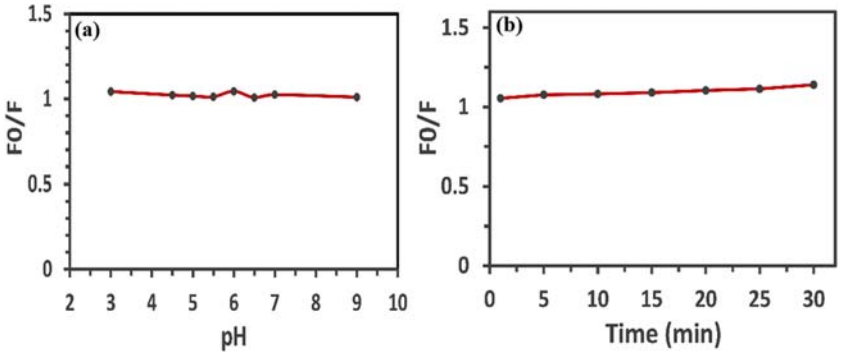

Fig. 7 (**a**) Fluorescence quenching efficiency F0/F of CDs by tartrazine in different pH buffers and (**b**) Fluorescence quenching efficiency F0/F of CDs by tartrazine during different time

hydrolyzed into glucose, which had been then dehydrated, polymerized, and forced to result in the formation of linear or branched oligosaccharides [43]. Once the procedure had reached a critical supersaturation, the linear or branched oligosaccharides of the solution has gone further through intermolecular dehydration and formed a cross-linked situation with each other, resulting in the bursts of rapid nucleation [44]. Eventually, we have obtained the desired fluorescence carbon dots particles and confirmed the existence of functional groups on their surface through the employment of FT-IR spectroscopy. Figure 9 demonstrates the probable mechanism of tartrazine detection based on the substances structural features. However, considering how the functional groups that exist on the surface of CDs have been confirmed by infrared spectroscopy, the formation of hydrogen bonds between tartrazine and CDs could be strongly assumed which belong to the surface group and can be observed in Fig. 9. Subsequent to the formation of hydrogen bonds, which reduces the distance between CDs and tartrazine, an opportunity for the occurrence of an electron transfer is facilitated that can lead to the inducement of fluorescence quenching.

Selectivity of CDs for Tartrazine Detection

The synthesized CDs have been settled to function in the role of fluorescent probe for the detection of tartrazine and for this purpose, first we had to be ensured that they would exhibit a selective behavior towards this synthetic dye. Recently, the selective detection of CDs through the usage of fluorescence probe has been the subject of several researches [27]. In order to study this selectivity method, the FL intensity changes in the presence of other different

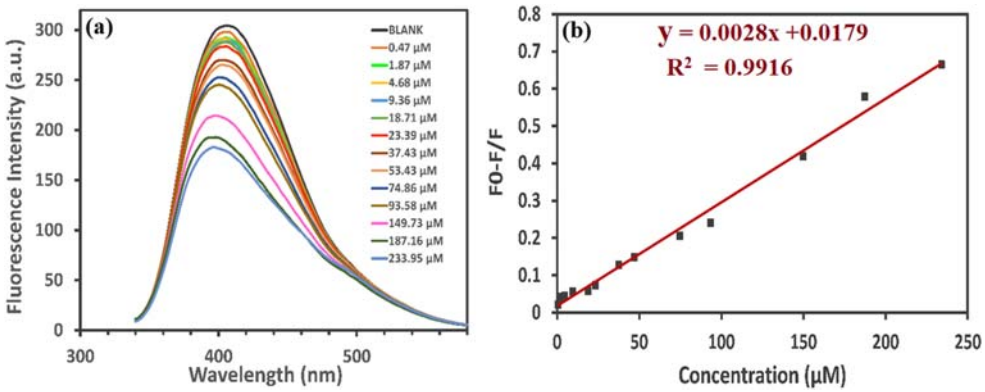

Fig. 8 (**a**) Fluorescence intensity of the CDs in the presence of different concentrations of tartrazine (from top to bottom, 0, 0.47, 1.87, 4.68, 9.36, 18.71, 23.39, 37.43, 53.43, 74.86, 93.58, 149.73, 187.16, 234 μM) and (**b**) Calibration curve

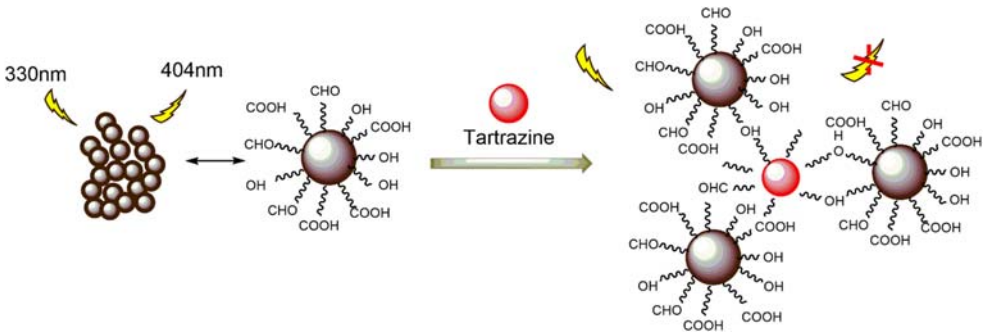

Fig. 9 The schematic diagram for the fluorescence of the CDs quenched by tartrazine

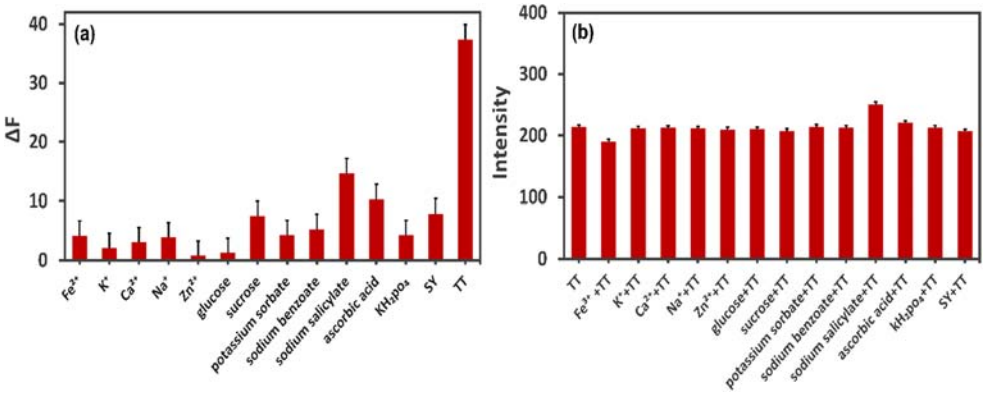

Fig. 10 (**a**) Selectivity of the developed sensing strategy for tartrazine compared to different substances and (**b**) Fluorescence intensity of CDs with tartrazine and competitive substances interference

substances, including Fe^{3+}, K^{+}, Ca^{2+}, Na^{+}, Zn^{2+}, glucose, sucrose, potassium sorbate, sodium benzoate, sodium salicylate, ascorbic acid, potassium dihydrogen phosphate, and sunset yellow has been investigated under the similar conditions that had been applied for tartrazine (all at the same concentrations). Being in accordance with Fig. 10a, the occurrence of a prominent intensity has been observed only from tartrazine, while there has not been any other notable alteration in the CDs as the other substances had been appended. We have also evaluated the interference of other competitive materials on the proposed method and for this purpose, similar substances along with tartrazine have been appended to the mixture. In comparison to the solo presence of tartrazine, the sensing system has exhibited little alterations in regard to FL intensity upon the addition of other materials even as the the interférences concentrations had been 4 times higher than that of the analyte tartrazine [42]. Therefore, it can be stated that this product can stand as a suitable candidate for being applied as a selective probe for tartrazine since the effect of these interfering materials can be neglected when being compared to the binding of tartrazine and CDs (Fig. 10b).

Application to Real Sample Analysis

We have assessed the practicality of the designed sensing system in detecting tartrazine throughout some real samples and to perform this analysis, different volumes of the standard tartrazine solution have been spiked into the designated food samples [45]. These testing samples has included ice cream and soft drink, since they commonly contain this synthetic dye as a colorant. The required samples have been procured from a local market in Mashhad, Iran, and the recovery portions have been distinguished in accordance with the following Eq. 3:

$$\text{Recovery}\ (\%) = (\text{found amount} - \text{detected amount})/\text{added amount} \times 100 \quad (3)$$

The relative recovery values of 95.12–106.69% have been achieved from the spiked samples that had been settled in three repeated measurements and the obtained outcomes have been indicative of the successful detection of tartrazine in real samples through the application of this method (Table 1).

Conclusions

This work has presented the development of a facile and one-step hydrothermal method for the synthesis of CDs through the usage of E.A., as a natural source. The synthesized CDs have exhibited an average size of 3.5 nm and had been observed to be well dispersed in water. The measured quantum yield of this product has been 16.8% and had involved the application of anthracene as a standard. The as-synthesized CDs have been successfully exerted in the role of a highly

Table 1 The analytical results for the analyzed samples

Samples	No.	Detected (μmol/L)	Added (μmol/L)	Found (μmol/L)	Recovery (%)	RSD (%)
Ice cream	1	ND[a]	15	14.42	96.16	1.08
	2	ND[a]	15	14.27	95.12	
	3	ND[a]	15	16.62	110.83	
Soft drink	1	ND[a]	56	54.33	97.01	2.28
	2	ND[a]	56	59.74	106.69	
	3	ND[a]	56	55.86	99.75	

[a] Not detectable

sensitive and selective fluorescent probe for the turn-off detection of tartrazine, while lacking the need for further chemical modifications. The gathered data from the performed analysis on food samples have been suggestive of the offered method practicality in real samples. In addition, this procedure has enhanced the application of CDs in the field of food monitoring due to containing a green, simple, and low-cost synthesizing procedure while offering a satisfying amount of selectivity and sensitivity.

Acknowledgements The authors gratefully acknowledge the technical support of this work that has been provided by Ferdowsi University of Mashhad and Mashhad University of Medical Sciences based on the Ph. D thesis of Mrs. M. Ghereghlou.

Author Contributions Mahnaz Ghereghlou: Writing original draft, synthesized and characterized the compounds using XRD, UV-Vis, TRM, FTIR techniques. Abbas Ali Esmaeili: Data acquisition, analysis and interpretation, review and editing, Funding and resources acquisition. Majid Darroudi: Supervision, Project administration, review & editing, Funding and resources acquisition.

Data Availability Not applicable.

Conflicts of Interest/Competing Interests

The authors have declared no conflict of interest.

Ethics Approval For this type of study, the ethical approval was not.

References

1. Xu L, Baldocchi DD, Tang J (2004) How soil moisture, rain pulses, and growth alter the response of ecosystem respiration to temperature. Glob Biogeochem Cycles 18(4)
2. Lim S, Wyker B, Bartley K, Eisenhower D (2015) Lim et al. respond to "measurement error and physical activity". Am J Epidemiol 181(9):659–660
3. Liu X, Xu W, Pan Y, Du E (2015) Liu et al. suspect that Zhu et al. (2015) may have underestimated dissolved organic nitrogen (N) but overestimated total particulate N in wet deposition in China. Sci Total Environ 520:300–301. https://doi.org/10.1016/j.scitotenv.2015.03.004
4. Schmitt A, Malchow B, Hasan A, Fallkai P (2014) The impact of environmental factors in severe psychiatric disorders. Front Neurosci 8:19
5. Zhang Q, Liang J, Zhao L, Wang Y, Zheng Y, Wu Y, Jiang L (2020) Synthesis of novel fluorescent carbon quantum dots from Rosa roxburghii for rapid and highly selective detection of o-nitrophenol and cellular imaging. Frontiers in chemistry 8:665
6. Rahnama A, Ramezani Z (2018) Carbon quantum dots in environmental remediation. International Journal of Environmental Sciences & Natural Resources 10(4):158–161
7. Edison AS, Hall RD, Junot C, Karp PD, Kurland IJ, Mistrik R, Reed LK, Saito K, Salek RM, Steinbeck C (2016) The time is right to focus on model organism metabolomes. Metabolites 6(1):8
8. Sahu SK, Thangaraj M (2012) Kathiresan K (2012) DNA extraction protocol for plants with high levels of secondary metabolites and polysaccharides without using liquid nitrogen and phenol. International Scholarly Research Notices
9. Niu K, Messier J, He J-S, Lechowicz MJ (2015) The effects of grazing on foliar trait diversity and niche differentiation in Tibetan alpine meadows. Ecosphere 6(9):1–15
10. Zhou X, Wildschut T, Sedikides C, Chen X, Vingerhoets AJ (2012) Heartwarming memories: nostalgia maintains physiological comfort: correction to Zhou et al
11. Xiang X, Piers TM, Wefers B, Zhu K, Mallach A, Brunner B, Kleinberger G, Song W, Colonna M, Herms J, Wurst W, Pocock JM, Haass C (2018) The Trem2 R47H Alzheimer's risk variant impairs splicing and reduces Trem2 mRNA and protein in mice but not in humans. Mol Neurodegener 13(1):49. https://doi.org/10.1186/s13024-018-0280-6
12. Liu C, Allan RP, Mayer M, Hyder P, Loeb NG, Roberts CD, Valdivieso M, Edwards JM, Vidale PL (2017) Evaluation of satellite and reanalysis-based global net surface energy flux and uncertainty estimates. Journal of Geophysical Research: Atmospheres 122(12):6250–6272
13. Surendran P, Lakshmanan A, Priya SS, Balakrishnan K, Rameshkumar P, Kannan K, Geetha P, Hegde TA, Vinitha G (2020) Bioinspired fluorescence carbon quantum dots extracted from natural honey: efficient material for photonic and antibacterial applications. Nano-Structures & Nano-Objects 24:100589. https://doi.org/10.1016/j.nanoso.2020.100589
14. Qu X, Su L, Li H, Liang M, Shi H (2018) Assessing the relationship between the abundance and properties of microplastics in water and in mussels. Sci Total Environ 621:679–686
15. Öztürk Hİ, Aydın S, Sözeri D, Demirci T, Sert D, Akın N (2018) Fortification of set-type yoghurts with Elaeagnus angustifolia L. flours: effects on physicochemical, textural, and microstructural characteristics. LWT 90:620–626
16. Khadivi A (2018) Phenotypic characterization of Elaeagnus angustifolia using multivariate analysis. Ind Crop Prod 120:155–161
17. Ghoreishi SM, Behpour M, Golestaneh M (2012) Simultaneous determination of sunset yellow and tartrazine in soft drinks using gold nanoparticles carbon paste electrode. Food Chem 132(1):637–641
18. Llamas NE, Garrido M, Di Nezio MS, Band BSF (2009) Second order advantage in the determination of amaranth, sunset yellow FCF and tartrazine by UV–vis and multivariate curve resolution-alternating least squares. Anal Chim Acta 655(1–2):38–42
19. El Rabey HA, Al-Seeni MN, Al-Sieni AI, Al-Hamed AM, Zamzami MA, Almutairi FM (2019) Honey attenuates the toxic effects of the low dose of tartrazine in male rats. J Food Biochem 43(4):e12780
20. Wang Y, Mu Y, Hu J, Zhuang Q, Ni Y (2019) Rapid, one-pot, protein-mediated green synthesis of water-soluble fluorescent nickel nanoclusters for sensitive and selective detection of tartrazine. Spectrochim Acta A Mol Biomol Spectrosc 214:445–450
21. Alp H, Başkan D, Yaşar A, Yaylı N, Ocak Ü, Ocak M (2018) Simultaneous determination of sunset yellow FCF, allura red AC, quinoline yellow WS, and tartrazine in food samples by RP-HPLC. Journal of Chemistry 2018:1–6
22. Hurst W, McKim J, Martin R Jr (1981) Determination of tartrazine in food products by HPLC. J Food Sci 46(2):419–420
23. Gianotti V, Angioi S, Gosetti F, Marengo E, Gennaro M (2005) Chemometrically assisted development of IP-RP-HPLC and spectrophotometric methods for the identification and determination of synthetic dyes in commercial soft drinks. J Liq Chromatogr Relat Technol 28(6):923–937
24. de Andrade FI, Guedes MIF, Vieira ÍGP, Mendes FNP, Rodrigues PAS, Maia CSC, Ávila MMM, de Matos RL (2014) Determination of synthetic food dyes in commercial soft drinks by TLC and ion-pair HPLC. Food Chem 157:193–198
25. Gan T, Sun J, Cao S, Gao F, Zhang Y, Yang Y (2012) One-step electrochemical approach for the preparation of graphene wrapped-

phosphotungstic acid hybrid and its application for simultaneous determination of sunset yellow and tartrazine. Electrochim Acta 74:151–157
26. Song Y, Xu J, Lv J, Zhong H, Ye Y, Xie J (2012) Electrochemical reduction of tartrazine at multi-walled carbon nanotube-modified pyrolytic graphite electrode. Russ J Phys Chem A 86(2):303–310
27. Thulasi S, Kathiravan A, Asha Jhonsi M (2020) Fluorescent carbon dots derived from vehicle exhaust soot and sensing of Tartrazine in soft drinks. ACS Omega 5(12):7025–7031. https://doi.org/10.1021/acsomega.0c00707
28. Banerjee T, Singh A, Sharma R, Maitra A (2005) Labeling efficiency and biodistribution of technetium-99m labeled nanoparticles: interference by colloidal tin oxide particles. Int J Pharm 289(1–2): 189–195
29. Yang X, Xu J, Luo N, Tang F, Zhang M, Zhao B (2020) N, Cl co-doped fluorescent carbon dots as nanoprobe for detection of tartrazine in beverages. Food Chem 310:125832
30. Sobhani R, Rezaei B, Shahshahanipour M, Ensafi AA, Mohammadnezhad G (2019) Simple and green synthesis of carbon dots (CDs) from valerian root and application of modified mesoporous boehmite (AlOOH) with CDs as a fluorescence probe for determination of imipramine. Anal Bioanal Chem 411(14):3115–3124
31. Yvon HJ (2012) A guide to recording fluorescence quantum yields. Middlesex, UK, HORIBA Jobin Yvon Inc
32. Shaikh AF, Tamboli MS, Patil RH, Bhan A, Ambekar JD, Kale BB (2019) Bioinspired carbon quantum dots: an antibiofilm agents. J Nanosci Nanotechnol 19(4):2339–2345
33. Yan F, Bai Z, Zu F, Zhang Y, Sun X, Ma T, Chen L (2019) Yellow-emissive carbon dots with a large stokes shift are viable fluorescent probes for detection and cellular imaging of silver ions and glutathione. Microchim Acta 186(2):1–11
34. Rao BS, Kumar BR, Reddy VR, Rao TS, Chalapathi G (2011) Preparation and characterization of CdS nanoparticles by chemical co-precipitation technique. Chalcogenide Lett 8(3):177–185
35. Sabouri Z, Fereydouni N, Akbari A, Hosseini HA, Hashemzadeh A, Amiri MS, Kazemi Oskuee R, Darroudi M (2019) Plant-based synthesis of NiO nanoparticles using salvia macrosiphon Boiss extract and examination of their water treatment. Rare Metals 39: 1134–1144. https://doi.org/10.1007/s12598-019-01333-z
36. Sabouri Z, Akbari A, Hosseini HA, Khatami M, Darroudi M (2020) Egg white-mediated green synthesis of NiO nanoparticles and study of their cytotoxicity and photocatalytic activity. Polyhedron: 114351
37. Song J, Li J, Guo Z, Liu W, Ma Q, Feng F, Dong C (2017) A novel fluorescent sensor based on sulfur and nitrogen co-doped carbon dots with excellent stability for selective detection of doxycycline in raw milk. RSC Adv 7(21):12827–12834
38. Sabouri Z, Akbari A, Hosseini HA, Hashemzadeh A, Darroudi M (2019) Bio-based synthesized NiO nanoparticles and evaluation of their cellular toxicity and wastewater treatment effects. J Mol Struct 1191:101–109. https://doi.org/10.1016/j.molstruc.2019.04.075
39. Otavo-Loaiza RA, Sanabria-González NR, Giraldo-Gómez GI (2019) Tartrazine removal from aqueous solution by HDTMA-Br-modified Colombian bentonite. The Scientific World Journal 2019
40. Chatzimitakos T, Kasouni A, Sygellou L, Avgeropoulos A, Troganis A, Stalikas C (2017) Two of a kind but different: luminescent carbon quantum dots from Citrus peels for iron and tartrazine sensing and cell imaging. Talanta 175:305–312
41. Niu X, Liu G, Li L, Fu Z, Xu H, Cui F (2015) Green and economical synthesis of nitrogen-doped carbon dots from vegetables for sensing and imaging applications. RSC Adv 5(115):95223–95229
42. Xu H, Yang X, Li G, Zhao C, Liao X (2015) Green synthesis of fluorescent carbon dots for selective detection of tartrazine in food samples. J Agric Food Chem 63(30):6707–6714
43. Wang Y, Wang K-M, Shen G-l, Yu R-Q (1997) A selective optical chemical sensor for o-nitrophenol based on fluorescence quenching of curcumin. Talanta 44(7):1319–1327
44. Guo L, Zeng X, Lan J, Yun J, Cao D (2017) Absorption competition quenching mechanism of porous covalent organic polymer as luminescent sensor for selective sensing Fe3+. ChemistrySelect 2(3):1041–1047
45. Wang Y, Zhu Y, Yu S, Jiang C (2017) Fluorescent carbon dots: rational synthesis, tunable optical properties and analytical applications. RSC Adv 7(65):40973–40989